

NASA Technical Memorandum 81388

**OPEN-CIRCUIT VOLTAGE IMPROVEMENTS
IN LOW RESISTIVITY SOLAR CELLS**

**M. P. Godlewski, T. M. Klucher,
G. A. Mazaris, and V. G. Weizer
Lewis Research Center
Cleveland, Ohio**

**Prepared for the
Fourteenth Photovoltaic Specialists Conference
sponsored by the Institute of Electrical and Electronics Engineers
San Diego, California, January 7-10, 1980**

**(NASA-TM-81388) OPEN-CIRCUIT VOLTAGE
IMPROVEMENTS IN LOW RESISTIVITY SOLAR CELLS
(NASA) 11 p HC A02/MF A01 CSCL 10A**

N80-15555

**Unclas
G3/44 46635**

OPEN-CIRCUIT VOLTAGE IMPROVEMENTS IN LOW RESISTIVITY SOLAR CELLS

by M. P. Godlewski, T. M. Klucher,
G. A. Mazaris, and V. G. Weizer

National Aeronautics and Space Administration
Lewis Research Center
Cleveland, Ohio 44135

ABSTRACT

Improvements in the open-circuit voltage of 0.1 ohm-cm silicon solar cells have been achieved using a multistep diffusion technique. Experimental details are given along with the results of an analysis that indicate that anomalous behaviors of the electron mobility in the cell base limits attainment of higher voltages.

INTRODUCTION

The Lewis Research Center has been engaged in an effort to identify the mechanisms limiting the open-circuit voltage (V_{oc}) in 0.1 ohm-cm, p-base solar cells. Theoretical estimates predict that voltages in the range $0.680 < V_{oc} < 0.700$ volts are possible. Initial attempts to produce cells with these voltages were unsuccessful, however, the highest voltages being about 610 volts. Recently several rather unorthodox approaches have succeeded in producing significant voltage increases. Figure 1 illustrates the present status of the various efforts. If we assume ideal diode characteristics and compare the voltages of these cells at arbitrary current density of $100 \text{ mA}/4 \text{ cm}^2$, we see that the highest voltage (0.648 V) was achieved by the University of Florida's epitaxially deposited, high low emitter (HLE) cell (1). Voltages in the 0.637 to 0.640 volt range were obtained by the Spire Corporation with their ion-implanted emitter (IIE) cell (2), by NASA-Lewis using a multistep diffusion (MSD) technique, and by the University of New South Wales with their MIS cell (3). These voltages represent a significant improvement over the 0.610 volt level that marked the best effort several years ago. At least in the case of the Lewis MSD cell, however, these experimental advances have preceded theoretical understanding in that we do not have a detailed knowledge of the mechanisms responsible for the increased voltages. Such knowledge is necessary if these processes are to be optimized and the maximum voltages realized. The purpose of this paper, therefore, is to describe the techniques used in the Lewis program and to present the results of an effort to identify the voltage limiting mechanisms operating in the Lewis MSD cell. The results of a similar effort to determine the voltage limiting mechanisms in the HLE cell and the IIE cell will also be presented.

It should be noted that throughout the remainder of the paper, the V_{oc} will be defined as the voltage obtained under illumination sufficient to produce a current density of $25 \text{ mA}/\text{cm}^2$.

EXPERIMENTAL

The Lewis multistep fabrication schedule is given in Table I along with a list of the best conditions found to date. The schedule consists of three steps, all of which have been found to be necessary. The first step is a high temperature (950°C) long time ($t > 4 \text{ hr}$) diffusion. This primary diffusion is followed by an acid-etch ($\text{HF}:\text{HNO}_3:\text{HAc}$) removal of the emitter surface such that the final sheet resistance is in the 10 to 12 ohm/ \square range. The etching step is then followed by a short, low temperature secondary diffusion. Final junction depths range from 1 to 4 micrometers. Both gaseous (PH_3) and spin-on doped oxide diffusion sources were used. I-V data were obtained with a xenon X-25 solar simulator. Diffusion lengths were measured using an X-ray technique and spectral response data were taken with a nine point narrow band filter wheel.

DETERMINATION OF THE VOLTAGE LIMITING MECHANISM

As stated above, the Lewis MSD schedule has not been completely optimized. Consider, for example, the times of primary diffusion. As shown in Fig. 2, we have found a direct correlation between the primary diffusion time and the open-circuit voltage. As can be seen, the highest voltage was obtained for the longest diffusion time attempted. These data suggest that the way to increased voltage is through further increases in diffusion time. As the diffusion time approaches 100 hours, however, not only does cell fabrication become unacceptably cumbersome, but current output is also reduced due to the increases in the junction depth. It was therefore decided to investigate the mechanisms involved with the voltage increases at hand. Identification of the controlling mechanism would hopefully enable achievement of further voltage increases in shallower junction cells. In the remainder of the paper, therefore, we will describe our efforts to determine the voltage controlling component of the device saturation current, and to identify the critical parameter in that component that limits further voltage increases.

Identification of the Voltage Limiting Saturation Current Component

The open-circuit voltage as defined in the introduction is determined by the value of the device saturation current density, I_0 . I_0 has, in general, three components: a base component, I_{0B} , an emitter component, I_{0E} , and a depletion region component, I_{0DR} . The first step in the search for the voltage limiting mechanism is to determine the relative magnitudes of each of these components. Since these cells all exhibit ideal diode characteristics in the voltage range near V_{oc} , we know that I_{0DR} is negligibly small. The relative degree of control exercised by the remaining two components can be determined by analyzing the results of some 1 MeV electron irradiation experiments. In these experiments, a number of typical cells were irradiated in steps to fluences of 1×10^{12} , 1×10^{13} , 3×10^{13} , 1×10^{14} , 3×10^{14} , and 1×10^{15} e/cm². At each fluence level the diffusion lengths, the current-voltage characteristics, and the spectral responses were measured. Figure 3 illustrates the behavior of the red (0.9 μ m) and the blue (0.5 μ m) monochromatic spectral responses when a cell which has received a 4 hour 950° C primary diffusion is subjected to 1 MeV electron irradiation. As can be seen, the red response is severely degraded by the irradiation, while the blue response is essentially unaffected. If we assumed that this invariance of the blue response with fluence indicates that I_{0E} is not affected by the irradiation, the task of separating base and emitter effects is greatly simplified.

In Fig. 4, for example, the V_{oc} of this same cell is plotted as a function of the base diffusion length. Since the magnitude of the decrease in the open-circuit voltage with decreasing base diffusion length depends on the value of I_{0E} , we should be able to determine I_{0E} (assumed constant) by fitting the appropriate theoretical expression to the data in Fig. 4. The expression for V_{oc} is given by

$$V_{oc} = \frac{kT}{q} \ln \left[I_{sc} \left(I_{0E} + \frac{A}{L} \coth \frac{d}{L} \right)^{-1} \right]$$

where

$$A = \frac{qn_1^2 D}{N_A}$$

I_{sc} is the short-circuit current density, T is the absolute temperature, L is the base diffusion length, n_1 is the intrinsic carrier concentration, D is the electron diffusivity, N_A is the boron concentration at the base depletion region edge, d is the cell thickness, k is Boltzmann's Constant, q is the electronic charge, and an ohmic rear contact is assumed.

A fit of Eq. (1) to the data in Fig. 4, using I_{0E} and A as adjustable parameter, is shown as the solid curve in that figure. The results of the fit indicate that the device saturation current before irradiation was composed of a 68% contribution

from the base and a 32% contribution from the emitter.

These results and the results the same analysis performed on cells diffused at the same temperature but for 16, 41, and 65 hours are summarized in Fig. 5, where the device saturation current and its components are plotted against primary diffusion time. In order to compare the variations in I_0 and its components independently of diffusion length differences, the data in this figure were obtained from Eq. (1) using the experimentally derived values of I_{0E} and A , and requiring the diffusion length to be 220 micrometers in all cases. Thus, any variations in I_0 must be ascribed to some parameter other than L .

Measurements similar to those made on the Lewis MSD cells were performed on a limited sampling of 11E and HLE cells in an attempt to determine the voltage controlling components of I_0 in each of these cases. An analysis of 1 MeV electron irradiation data for the ion-implanted cells indicated that the voltage in this type of cell, as in the Lewis cell, is controlled by I_{0B} . The results for one 11E cell are plotted in Fig. 5.

An inspection of Fig. 5 indicates that in all cases, I_{0B} is the dominant component. I_{0E} , while contributing to the total saturation current, appears to remain constant with diffusion time. The voltage increases observed with increase in diffusion time can therefore be attributed to decreases in I_{0B} :

Because of the complexity of the HLE cell (1), an analysis similar to that performed above is not possible. Since both the blue and the red spectral response components were found to be degraded by electron irradiation, an assumption of constant I_{0E} cannot be made. The diffusion lengths in both regions are apparently a function of fluence. While a quantitative analysis of these cells would be difficult, some qualitative conclusions can be drawn. Figure 7 shows the experimental V_{oc} vs. fluence data for the HLE cell. Superimposed on these data is a curve illustrating what would be expected if the voltage of this cell were controlled only by the radiation induced decrease in the base diffusion length. As can be seen, the measured decrease in the base diffusion length can account for only a small fraction of the observed voltage drop. We can thus conclude that the voltage is controlled to a high degree by the emitter component of the device saturation current.

Further evidence of base control in the MSD cells is obtained from the relationship between the V_{oc} and spectral response. Figure 6 shows the relationship between the V_{oc} and the monochromatic 0.5 and 0.9 μ m spectral responses for a large number of cells fabricated with 4 hours, 950° C primary diffusions. The assumption made here is that the parameters affecting the current output from a given region of the cell (i.e., the base or the emitter) will also affect the value of the saturation current in that region. Therefore, if I_{0B} were controlling the voltage, we would expect a positive correlation between the base current

(0.9 μm response) and the V_{oc} . The fact that Fig. 6 shows such a correlation supports the previous base control conclusions. The lack of correlation between the voltage and the emitter current (0.5 μm response) is also consistent with base control.

To summarize, the preceding data suggest strongly that the open-circuit voltages both in the Lewis MSD cells and the Spire HLE cells are controlled by the base component of the device saturation current. In the Florida HLE cells, on the other hand, the emitter appears to be controlling.

Determination of the Critical Voltage Limiting Parameter

The previous results strongly indicate that I_{OB} controls the V_{oc} in the Lewis MSD cells. The next step is to identify the parameter in I_{OB} that is influenced by the diffusion time in such a way as to produce higher voltages as the diffusion time is increased.

I_{OB} can be expressed as

$$I_{OB} = \frac{q n_i^2 D}{N_A L} \coth \frac{d}{L} \quad (3)$$

In an attempt to isolate the voltage controlling parameter in Eq. (3), a number of cells were selected that had widely different open-circuit voltages but nearly identical base diffusion lengths, thicknesses, and rear surface treatments. The primary diffusion times for these cells were 4, 16, and 41 hours. It is reasoned that, since all other parameters were identical, the voltage differences between these cells must be due to differences in either the base dopant (boron) concentration and/or profile, or the base minority carrier diffusivity.

The electrically active boron concentration profiles on the base side of the junction can be obtained by measuring the phosphorus concentration and subtracting it from the pre-diffusion boron concentration which is assumed constant since all these cells were fabricated from the same ingot. The phosphorus concentrations were determined through SIMS measurements. The results are shown in Fig. 8. As can be seen, the profiles are unexpectedly similar in the vicinity of the junction. With the assumption that this similarity extends beyond the junction into the base region, we find that the calculated boron profiles in that layer are identical.

We can conclude, therefore, that because the net boron profiles, the base diffusion lengths, the thicknesses, and the rear surface recombination velocities of these cells are identical, their observed voltage differences must be due to differences in the remaining variable (i.e., the base region minority carrier diffusivity). To explain the observed voltage increases, one would have to invoke a reduction in the diffusivity as the diffusion time is increased.

The validity of these conclusions could be tested through a measurement of the base diffusivity of these three cells. Theoretically this could be done by making independent measurements of the diffusion length and the lifetime and employing the well known relation, $L = D\tau$, where τ is the base minority carrier lifetime. Unfortunately, attempts to measure τ in the above cells using an open-circuit voltage decay (OCVD) technique were unsuccessful because of ambiguities in the interpretation of the decay curves. We can, however, present some auxiliary evidence to attest to the existence of large changes in minority carrier diffusivity with diffusion time.

The data presented in Table II were obtained at Lewis several years ago during a study of shallow junction, 10 ohm-cm devices. It can be seen that as the diffusion time was increased, the diffusion lengths decreased significantly. However, contrary to what would be expected, as the diffusion length decreased, the open-circuit voltage increased. To investigate the cause of this strange behavior, the lifetimes of these cells were measured using an OCVD technique, and the diffusivities calculated using Eq. (2). The results, shown in Table II, indicate a large drop in the value of D as the diffusion time was increased from 30 minutes to 2 hours. These variations in diffusivity with diffusion time are very similar to what has been observed in the present MSD cells. It appears reasonable, therefore, on the basis of the above data, to ascribe the voltage limiting role in Lewis MSD cells to the electron diffusivity in the cell base.

DISCUSSION

The preceding analysis suggests that for short primary diffusions the electron diffusivity in the base of an MSD cell is anomalously high and, as the diffusion time is lengthened, the diffusivity decreases. Calculated mobility values for the three cells in Fig. 8, for instance, are 2170, 1490, and 1242 $\text{cm}^2/\text{V sec}$ for the 4, 16, and 41 hour diffused cells, respectively. These values are considerably higher than the 600 $\text{cm}^2/\text{V sec}$ value expected for 0.1 ohm-cm material. One possible explanation for this behavior is based upon piezoresistivity effects (i.e., on the effect of diffusion induced stresses on the diffusivity).

It is well known that the mobility, μ , in the silicon lattice (related to the diffusivity through the relation $D = kT\mu/q$) is a function of mechanical stresses applied to the crystal (4). It is also known that the diffusion of a high concentration of phosphorus into the silicon lattice produces large stresses in the lattice (5). It has been shown that these stresses exist not only in the diffused region, but extend for considerable distances ($>100 \mu\text{m}$) into the cell base as evidenced by the distribution of diffusion induced dislocations (6,7). It is suggested that the anomalous mobility behavior arises from the action of these stresses.

The composition of the stress fields in the base requires some comment. Since the diffusing

species are atomically smaller than the host lattice atoms, the diffused region of the crystal tends to contract. This contraction puts the adjacent regions of the lattice under compressive stress. While the contraction in the diffused region is hydrostatic, the stresses in the base are essentially two dimensional, existing only in directions parallel to the diffusion front. Furthermore, as far as the electrical characteristics of the cell are concerned, the important mobility component is that component perpendicular to the junction and thus transverse to this compressive stress field.

Fortunately there is some information in the literature describing the variation of the transverse component of the electron mobility in silicon as a function of a one-dimensional compressive stress (8). Extrapolation of these data to the room temperature fracture stress for silicon (9) indicates that mobility values as high as $2500 \text{ cm}^2/\text{V sec}$ should be possible. On the basis of these data, then, it is tempting to speculate that the anomalously high values of mobility in the short diffusion time cells are due to high, diffusion-induced lattice stresses in the base region. It can be further speculated that these stresses are relieved somewhat as the diffusion time is increased, thus lowering the mobility and providing increased voltages. According to this reasoning, the greater the lattice disturbances in the base region the lower the voltage from that cell.

In addition to the above, there is another piece of evidence to indicate that the high voltages achieved in these cells are associated with improvements in the lattice perfection of the base region. Two groups of MSD cells were fabricated, one of which was not acid etched between diffusions. The photon degradation phenomenon (10) was then used as a diagnostic tool to detect the presence or absence of lattice damage in the base as a function of the presence or absence of the acid etching step. The results indicated that emitter etching not only removes the highly damaged regions near the emitter surface, but that it also removes lattice damage from the base region.

It can be concluded, therefore, that the voltage controlling base region in these cells is strongly affected by the processing steps used to fabricate the emitter.

SUMMARY

The results of this study can be summarized as follows:

1. The open-circuit voltages of the Lewis MSD cell and the Spire 11E cell are controlled by the base component of the device saturation current, whereas the voltage of the Florida HLE cell is controlled by the emitter component.

2. The critical voltage limiting parameter in the Lewis MSD cell appears to be the electron mobility in the cell base.

3. Qualitative evidence suggests that the anomalous behavior of the base mobility may be explained in terms of the piezoresistive effects of stress fields existing in the base due to the presence of large concentrations of diffusant atoms in the emitter.

REFERENCES

1. F. A. Lindholm and A. Neugroschel, "Studies of Silicon PN Junction Solar Cells," University of Florida, Gainesville, FL, TR-78-1, 1978.
2. J. Minnucchi, "Study Program to Improve the Open Circuit Voltage of Low Resistivity Single Crystal Silicon Solar Cells," Spire Corp., Bedford, MA, MR-10056-07, 1979.
3. R. B. Godfrey and M. A. Green, "655 mV Open-Circuit Voltage, 17.6% Efficient Silicon MIS Solar Cells," *Appl. Phys. Lett.*, vol. 34, no. 11, pp. 790-793, June 1, 1979.
4. W. Paul and D. M. Warschauer, *Solids under Pressure*. New York: McGraw-Hill, 1963, p. 179.
5. G. H. Schwuttke and H. J. Queisser, "X-Ray Observations of Diffusion-Induced Dislocations in Silicon," *J. Appl. Phys.*, vol. 33, pp. 1540-1542, April 1962.
6. J. E. Lawrence, "Diffusion-Induced Stress and Lattice Disorders in Silicon," *J. Electrochem. Soc.*, vol. 113, pp. 819-824, August 1966.
7. I. M. Sukhodreva, "Observation of Dislocations Formed during Diffusion of Phosphorus into Silicon by the Anomalous X-Ray Transmission Method," *Sov. Phys. Solid State*, vol. 2, pp. 311-313, August 1964.
8. M. W. Cresswell and D. R. Muss, "Uniaxial Stress in Silicon and Germanium; Volume 1, Sections 1 and 2 and Volume 2, Sections 3-6," Westinghouse Electric Corp., Pittsburgh, PA, AFML-TR-68-124, V.1, Sec.1-2 and AFML-TR-68-124, V.2, Sec.3-6, 1968. (AD-835764 and AD-835765)
9. G. I. Pearson, W. T. Read, Jr., and W. L. Feldmann, "Deformation and Fracture of Small Silicon Crystals," *Acta Metall.*, vol. 5, pp. 181-191, 1957.
10. V. G. Weizer, H. W. Brandhorst, J. D. Broder, R. E. Hart, and J. H. Lamneck, "Photon-Degradation Effects in Terrestrial Silicon Solar Cells," *J. Appl. Phys.*, vol. 50, no. 6, pp. 4443-4449, June 1979.

TABLE I. - THE LEWIS MSD FABRICATION SCHEDULE

1. Primary diffusion

Surface concentration $1 \times 10^{20} \text{ cm}^{-3}$
 Temperature 950° C
 Time $>65 \text{ hr}$

2. Emitter etch

Sheet resistance 10-12 ohm/

3. Secondary diffusion

Surface concentration $\sim 2 \times 10^{20} \text{ cm}^{-3}$
 Temperature 750° C
 Time 15 min

TABLE II. - THE EFFECT OF DIFFUSION TIME

ON MINORITY CARRIER DIFFUSIVITY

Diffusion conditions, min	$V_{oc}^{25},$ V	$L^{(a)},$ μm	$\tau^{(b)},$ μsec	$D(\tau),$ cm^2/sec
750 - 30	0.523	120	2.0	72.0
750 - 60	.524	70	2.0	24.5
750 - 120	.527	36	2.3	5.6

(a) X-ray technique.

(b) OCVD technique.

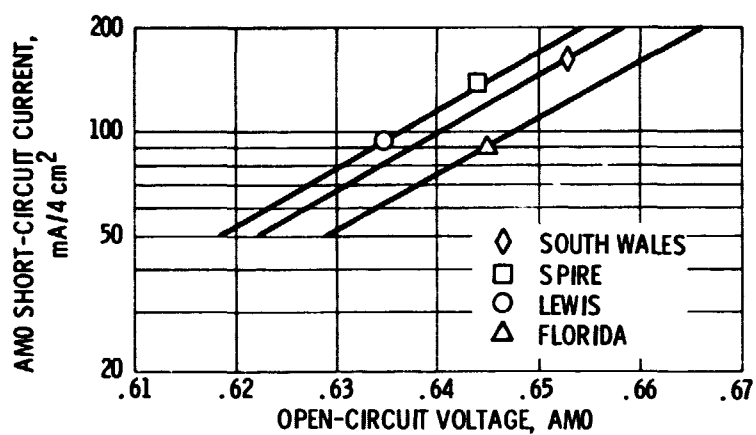


Figure 1. - Comparison of voltage improvements in 0.1 ohm-cm silicon cells.

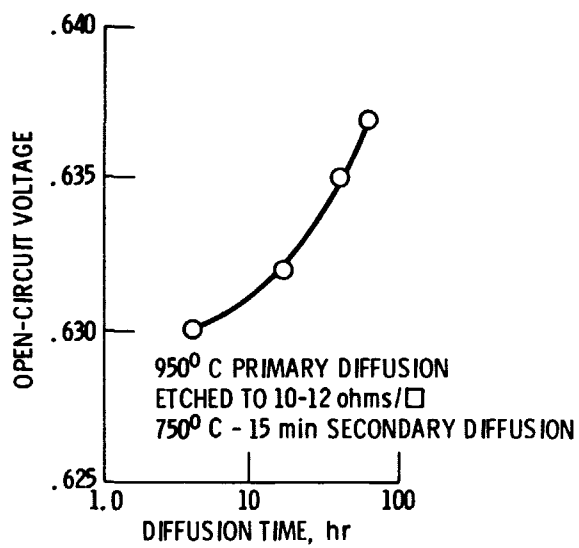


Figure 2. - Open-circuit as a function of primary diffusion time.

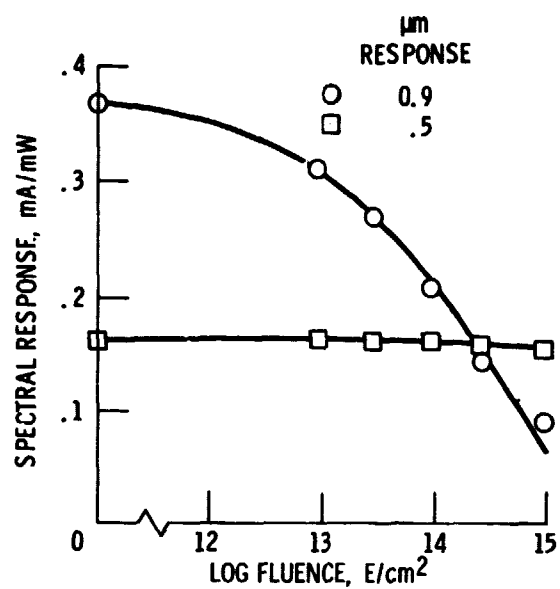


Figure 3. - Effect of 1 MeV electron irradiation on red (0.9 μm) and blue (0.5 μm) spectral responses.

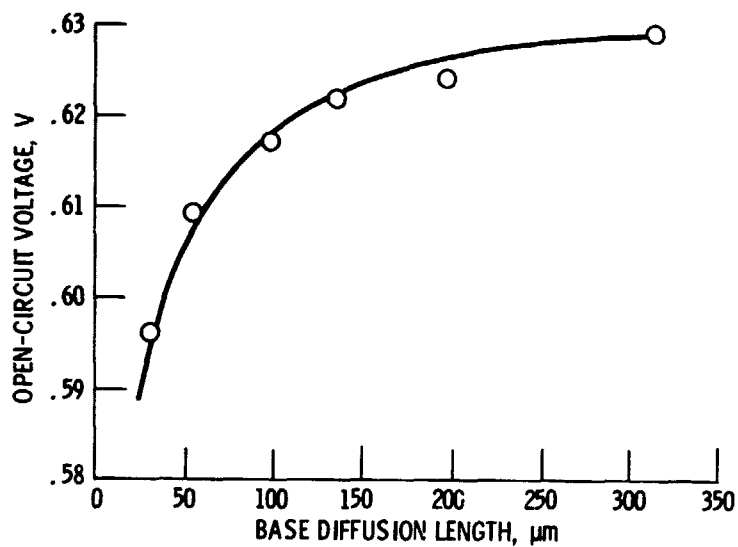


Figure 4. - Influence of base diffusion length on open-circuit voltage.

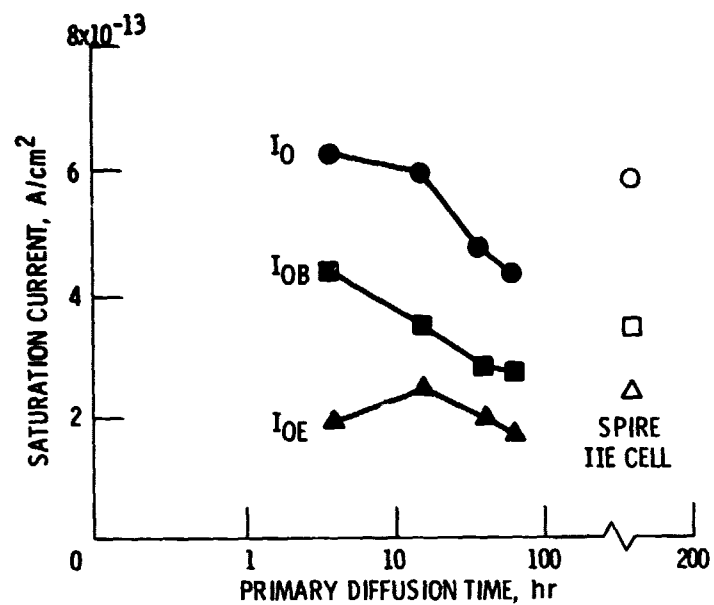


Figure 5. - Variation of device saturation current and its components with primary diffusion time.

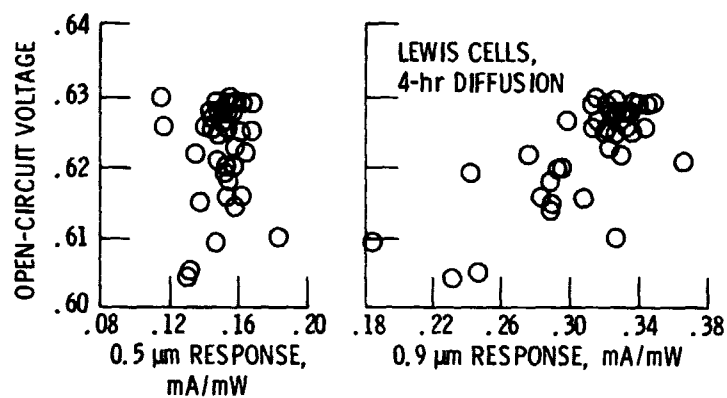


Figure 6. - Correlation between voltage and current for selected wavelengths.

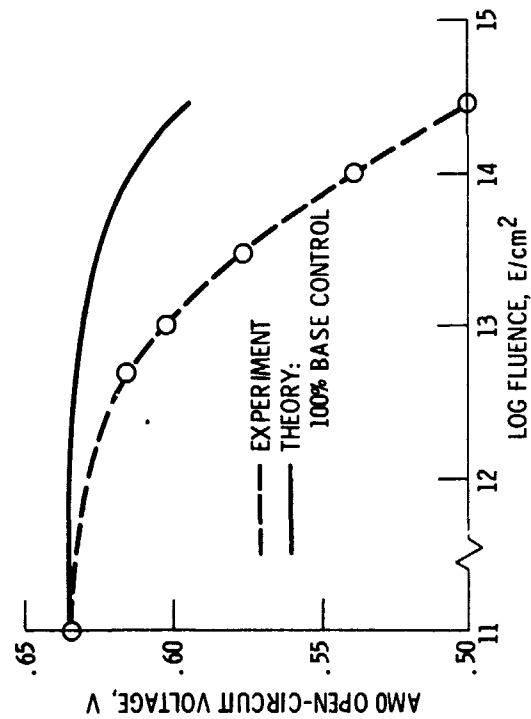


Figure 7. - Effect of 1 MeV electron irradiation on open-circuit voltage of a University of Florida HLE cell.

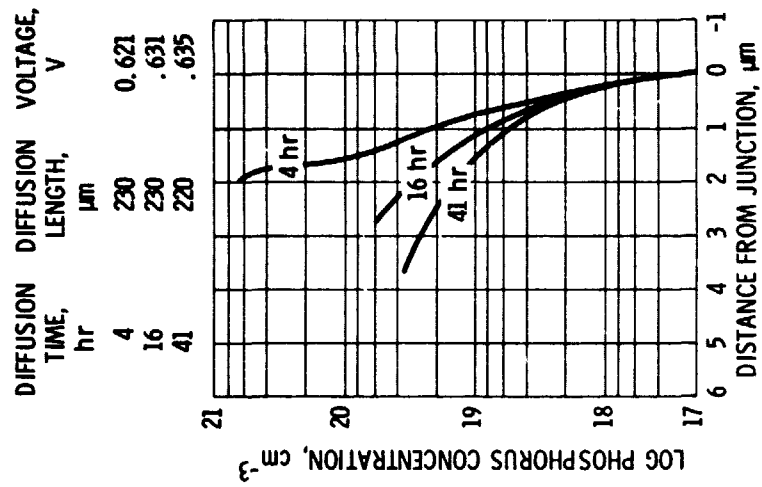


Figure 8. - Effect of primary diffusion time on phosphorus concentration profile (SIMS).

1. Report No. NASA TM-81388		2. Government Accession No.		3. Recipient's Catalog No.	
4. Title and Subtitle OPEN-CIRCUIT VOLTAGE IMPROVEMENTS IN LOW RESISTIVITY SOLAR CELLS				5. Report Date	
				6. Performing Organization Code	
7. Author(s) M. P. Godlewski, T. M. Klucher, G. A. Mazaris, and V. G. Weizer				8. Performing Organization Report No. E-298	
9. Performing Organization Name and Address National Aeronautics and Space Administration Lewis Research Center Cleveland, Ohio 44135				10. Work Unit No.	
				11. Contract or Grant No.	
12. Sponsoring Agency Name and Address National Aeronautics and Space Administration Washington, D.C. 20546				13. Type of Report and Period Covered Technical Memorandum	
				14. Sponsoring Agency Code	
15. Supplementary Notes					
16. Abstract <p>Improvements in the open-circuit voltage of 0.1 ohm-cm silicon solar cells have been achieved using a multistep diffusion technique. Experimental details are given along with the results of an analysis that indicate that anomalous behaviors of the electron mobility in the cell base limits attainment of higher voltages.</p>					
17. Key Words (Suggested by Author(s)) Solar cell Silicon Open circuit voltage				18. Distribution Statement Unclassified - unlimited STAR Category 44	
19. Security Classif. (of this report) Unclassified		20. Security Classif. (of this page) Unclassified		21. No. of Pages	
				22. Price*	

* For sale by the National Technical Information Service, Springfield, Virginia 22161